Atmos. Chem. Phys. Discuss., 8, 2715–2744, 2008
www.atmos-chem-phys-discuss.net/8/2715/2008/


Atmospheric Chemistry and Physics Discussions

# Nanoparticle formation in the exhaust of vehicles running on ultra-low sulfur fuel

**Hua Du and Fangqun Yu**

Atmospheric Sciences Research Center, State University of New York at Albany, New York 12203, USA

Received: 3 January 2008 – Accepted: 3 January 2008 – Published: 12 February 2008

Correspondence to: Hua Du (huadu@asrc.cestm.albany.edu )

Published by Copernicus Publications on behalf of the European Geosciences Union.



**Abstract**

The concern of adverse health impacts from exposure to vehicle-emitted nanoparticles has been escalating over the past few years. In order to meet more stringent EPA emission standards for particle mass emissions, advanced exhaust after-treatment systems such as continuously regenerating diesel particle filters (CRDPFs) have to be employed on vehicles and fuel with ultra-low sulfur is to be used. Although CRDPFs were found to be effective in reducing particle mass emissions, they were revealed to increase the potential of volatile nanoparticle formation. Significant nanoparticle concentrations have also been detected for vehicles running on ultra-low sulfur fuel but without CRDPFs. The main focus of this paper is the formation and evolution of nanoparticles in exhaust plume under ultra-low sulfur condition. Such study is necessary to project future nanoparticle emissions as fuel compositions and after-treatment systems change. We have carried out a comprehensive quantitative assessment of the effects of enhanced sulfur conversion efficiency, sulfur storage/release, and presence of non-volatile cores on nanoparticle formation using a detailed composition resolved aerosol microphysical model with a recently improved $H_2SO_4$-$H_2O$ homogeneous nucleation (BHN) module. Two well-controlled case studies show good agreement between model predictions and measurements in terms of particle size distribution and temperature dependence of particle formation rate, which leads us to conclude that BHN is the main source of nanoparticles for vehicles equipped with CRDPFs. We found that the employment of CRDPFs may lead to the higher number concentration of nanoparticles (but smaller size) in the exhaust of vehicles running on ultra-low sulfur fuel compared to those emitted from vehicles running on high sulfur fuel. We have also shown that the sulfate storage and release effect can lead to significant enhancement in nanoparticle production under favorable conditions. For vehicles running on ultra-low sulfur fuel but without CRDPFs, the BHN is negligible; however, the condensation of low volatile organic compounds on nanometer-sized non-volatile cores may explain the observed nucleation mode particles.

## 1 Introduction

Vehicle emission is one of the major sources of nanoparticles in urban areas. A large number of studies in the past few years have associated nanoparticles with adverse public health effects (Wold et al., 2006; Carbajal-Arroyo et al., 2007; Gauderman et al., 2007; Meng et al., 2007; Rundell et al., 2007). Therefore, a clear understanding of on-road nanoparticle formation and subsequent near-road evolution is critically important for the quantitative assessment of nanoparticle exposure levels to travelers on roadways and residents living nearby. Diesel vehicles are known to be one of the major sources of the particulate matter near busy roads. Recently, continuously regenerating diesel particle filters (CRDPFs) have been shown to be able to reduce particulate matter emission by orders of magnitude. However, their effect on the nanoparticle formation remains unclear. It is also important to know the extent to which CRDPF affects the production of nanoparticle formed via the combustion of ultra-low sulfur fuels.

Nanoparticle formation in vehicular exhaust is a complex process whose rates depend strongly on a number of factors including the sulfur content in fuel and lubricating oil, engine operation conditions, exhaust after-treatment setups, ambient conditions and exhaust dilution. Binary $H_2SO_4$-$H_2O$ homogeneous nucleation (BHN) theory has been applied to study nucleation in diesel exhaust. It has been shown that in the high sulfur fuel conditions (i.e. fuel sulfur content (FSC)>300 ppm), BHN may account for formation of vehicle-emitted nanoparticles (Du and Yu, 2006). Lemmetty et al. (2006) also applied a classical BHN model to study maximum $H_2SO_4$-$H_2O$ nucleation rates in the diesel exhaust assuming the sulfur to sulfuric acid conversion efficiency of 100% and exhaust temperature of ∼400 K. It is important to note that Lemmetty et al. (2006) may have over predicted maximum nucleation rates because the exhaust temperature of >∼700 K is needed in order to achieve a 100% conversion efficiency (Giechaskiel et al., 2007).

At the present time, the fuel sulfur content (FSC) for diesel vehicles has been reduced from ∼500 ppm to 15 ppm (by weight) nationwide. The role of BHN in nanoparticle formation in ultra-low sulfur conditions (i.e., FSC ∼15 ppm) is expected to be negligible (Du and Yu, 2006) due to the nonlinear dependence of nucleation rates on $H_2SO_4$ concentration,. However, many recent laboratory experiments and in situ measurements have shown that number concentrations of nanoparticles emitted by vehicles running on the ultra-low sulfur fuel are unexpectedly high (Maricq et al., 2002; Vaaraslahti et al., 2004; Vaaraslahti et al., 2005; Arnold et al., 2006; Kittelson et al., 2006; Giechaskiel et al., 2007; Rönkkö et al., 2007). This suggests that the application of CRDPFs may have profound effects on the observed nanoparticle formation. In the presence of CRDPFs, the nucleation mode was found to be sensitive to FSC and the most (∼90%) mass of nucleation mode particles were found to be sulfate (Kittelson et al., 2006). This suggests that BHN may be involved in the nanoparticle formation mechanism under the aforementioned conditions. Two possible reasons for the influence of CRDPFs on nanoparticle formation can be identified : (a) enhanced sulfur conversion efficiency ($\varepsilon$) due to CRDPFs (Maricq et al., 2002; Vaaraslahti et al., 2004; Arnold et al., 2006; Kittelson et al., 2006; Giechaskiel et al., 2007); (b) sulfur storage/release effect (Arnold et al., 2006; Giechaskiel et al., 2007). On the other hand, in the absence of CRDPFs the number concentration of the nucleation mode particles was found to be independent of FSC (Vaaraslahti et al., 2004; Rönkkö et al., 2007). The sampled nanoparticles were shown to have non-volatile cores coated with organics (Rönkkö et al., 2007). Although numerous experimental studies have demonstrated the importance of different factors on the nanoparticle production, the formation mechanisms behind the elevated nanoparticle production remain elusive. In the present paper, the effect of the above-mentioned factors (enhanced sulfur conversion efficiency, sulfur storage/release, and presence of non-volatile cores) on the nanoparticle formation in the presence or absence of CRDPFs has been studied using the size and composition resolved aerosol microphysical model. The major objective of the present study is to investigate the formation mechanism for nanoparticles emitted by vehicles running on ultra low sulfur fuel by focusing on the effects of the enhanced sulfur conversion efficiency, sulfur storage/release, and presence of non-volatile cores.

## 2 Method

1. Dilution of exhaust plume in the atmosphere

In order to study the nanoparticle formation and evolution inside a single vehicular plume, the size and composition resolved aerosol model has been developed. There are three distinct stages for the evolution of the vehicular plume, which are characterized by different dilution and dominant aerosol microphysical processes. The stage 1 starts at 0 s (right behind the tailpipe) and ends at 1 s of the plume age. The plume age is defined as time elapsed after the exhaust is emitted from the tailpipe. The hot vehicular exhaust experiences rapid dilution due to strong turbulence in the near field of the tailpipe. At this stage of the plume evolution, the nucleation is the key microphysical process. Studies (Kittelson et al., 1988; Shi et al., 2002) have shown that typical dilution ratios at this stage are ∼1000. The dilution ratio as a function of the plume age used in this study was obtained using the nonlinear regression of the experimental data by Kittelson et al. (1988). The dilution ratio ($DR$) in Kittelson et al. (1988) is expressed as $DR=1.0+700\times t^{1.413}$ ($t\leq 1$ s).

The stage 2 begins after 1s and ends when the exhaust reaches the roadside. At this stage the low volatile organics still condense onto nucleated particles; however, semi-volatile organics may begin to evaporate due to dilution (Sakurai et al., 2003). The precise determination of the dilution ratio in a single on-road vehicle plume is a complex problem, whose solution requires accurate accounting for the vehicle generated turbulence and mixing of the considered plume with other plumes. At the present time, no commonly accepted dispersion model that could predict, with considerable degree of confidence, the on-road dilution profile for a single plume is available. In the present study, the dilution profile during the stage 2 was determined as the ratio of $CO_2$ concentration in raw exhaust before dilution to the observed on-road one. Typically, the dilution ratio at plume age of ∼5 s varies from ∼5 to∼10 (relative to $t=1$ s), depending on traffic density, wind speed and atmospheric stability.

The stage 3 occurs in the vicinity of the roadway (from roadside to any downwind



location perpendicular to the roadway). The aerosol processing at stage 3 involves coagulation, dilution, and evaporation of organics. The corresponding dilution profile can be determined from CO measurements. The additional dilution (relative to $t=5$ s) is assumed to be ∼10 at 150 m away from the roadside (Zhu et al., 2002).

### 2.1 Nanoparticle nucleation and evolution: a kinetic modeling

A discrete-sectional bin structure (Yu, 2006) is used to represent the size spectra of molecular clusters/particles ranging from molecular size to several micrometers. The formation and evolution of clusters/nanoparticles are simulated kinetically by solving the following set of differential equations (Yu, 2006),

$$\frac{\partial C_{i,X}}{\partial t} = I_{i+1,i}\delta_{X,A}\gamma_{i+1,X}C_{i+1,X} - I_{i,i-1}\gamma_{i,X}C_{i,X} + \sum_{j=1}^{i}\sum_{k=1}^{i-1} f_{j,k,i}\beta_{j,k}N_jC_{k,X} - C_{i,X}\sum_{j=1}^{i\,\max}\left(1-f_{i,j,i}\right)\beta_{i,j}N_j \quad (1)$$

where $i$, $j$, $k$ are bin indices, $C_{i,X}$ is the volume concentration of component $X$ (=$H_2SO_4$, $H_2O$, and other species including organics, soot and refractory cores) at bin $i$, $N_j$ is the number concentration of cluster/particle at bin $j$, $\beta_{i,j}$ is the coagulation kernel between particles at bin $i$ and bin $j$, $\gamma$ is the cluster evaporation rate, $i_{\max}$ is maximum number of bins in the model (set to be 150 in this study), $f_{j,k,i}$ is the volume fraction of intermediate particles (volume=$v_j+v_k$) partitioned into bin $i$, $I_{i+1,i}=\frac{v_1}{v_{i+1}-v_i}$ is the volume fraction of intermediate particles of volume $v_{i+1}-v_{1,A}$ partitioned into bin $i$, and$\delta_{X,A}$ accounts for the volume of $H_2SO_4$ molecules evaporated from the clusters, and is defined as

$$\delta_{X,A} = \begin{cases} v_i/v_{i+1}, & \text{if } X = H_2SO_4 \\ 1, & \text{if } X \neq H_2SO_4 \end{cases} \quad (2)$$

In present study, sulfuric acid and water are the only species involved in nucleation. Organics contribute to the aerosol formation via the condensation onto the nucleated particles. The improved kinetic quasi-unary nucleation (KQUN) model (Yu, 2007), in which measured thermochemical properties of $H_2SO_4$ monomers with hydrated sulfuric acid dimers and trimers (Hanson and Lovejoy, 2006) and data from two independent measurements of monomer hydration have been incorporated, has been employed. The improved KQUN model is thermodynamically more robust, and predicts binary homogeneous nucleation rates in good agreement with available experimental data. Another advantage of the aforementioned model is that the nanoparticle formation and subsequent evolution are coupled. The coupling allows explicit simulations of the aerosol dynamics (i.e. nucleation, coagulation and condensation) of vehicle-emitted nanoparticles on and near the roadway. It is important to note that previous theoretical studies on the nanoparticle evolution considered the latter two processes only and that the nucleation process was excluded from their models (Zhang et al., 2004; Jacobson et al., 2005).

Ambient background aerosols were included in our model, and they participate in scavenging of small nanoparticles and $H_2SO_4$ vapor molecules as exhaust mixes with the ambient air. The mean size and undiluted concentration of the background aerosols is assumed to be ~60 nm in diameter and $10^4$($cm^{-3}$), respectively (Kittelson et al., 2004). The mean size and concentration of soot particles is assumed to be 50 nm in diameter and $10^7 cm^{-3}$, respectively (Kittelson et al., 2004).

### 2.2 Organic condensation

The volume concentration change of organics (X=organics) due to cluster/particle condensation and evaporation is calculated using the following set of equations,

$$\frac{\partial C_{i,\mathrm{org}}}{\partial t} = \pi V_{\mathrm{org}} f_{\mathrm{corr}} N_i r_i^2 \nu_{\mathrm{org}} (P_{\mathrm{org}} - P_{s,\mathrm{org}} A_{\mathrm{kelvin}}) \quad (3)$$



$$f_{\mathrm{corr}} = \frac{kn_i}{0.75 + kn_i} \quad (4)$$

$$A_{\mathrm{kelvin}} = \exp\left(\frac{2\sigma_{\mathrm{org}} \nu_{\mathrm{org}}}{kTr_i}\right) \quad (5)$$

where $V_{\mathrm{org}}$, $\nu_{\mathrm{org}}$, $P_{\mathrm{org}}$, $P_{s,\mathrm{org}}$, and $\sigma_{\mathrm{org}}$ are the thermal speed, volume, vapor pressure, saturation vapor pressure, and surface tension of condensing organic species, respectively. $f_{\mathrm{corr}}$ is the correction factor accounting for the transition regime (Seinfeld and Pandis, 1998). $A_{\mathrm{kelvin}}$ is the Kelvin effect and $r_i$ is the wet radius of clusters/particles in bin $i$.

Two types of organics, low volatile from lubricating oil and semi-volatile from fuel, were treated within each size bin. Their surrogates are alkanes, which have been shown to be important for the diesel exhaust evolution (Sakurai et al., 2003). The vapor pressures of these surrogates are similar to those of alkenes of the same carbon number (Makar, 2001). Although there are probably hundreds of organic species in the vehicular exhaust, they can be divided into the two distinct categories, and the characterization of the organics using the above-mentioned criteria should not largely affect the major conclusions concerning the nanoparticle evolution.

## 3 Results

### 3.1 Effect of enhanced sulfur conversion efficiency on nanoparticle formation

One possible explanation of the nanoparticle formation under ultra-low sulfur fuel conditions is the enhanced sulfur conversion efficiency. The oxidation catalyst in the CRDPFs, for instance, not only oxidizes soot and other hydrocarbons to $CO_2$, but also converts significantly more $SO_2$ into $SO_3$. The $SO_3$ then reacts with $H_2O$ to form $H_2SO_4$. Thus, sulfur conversion efficiency can be considerably enhanced due to CRDPFs.

Sulfur conversion efficiency $\varepsilon$ of after-treatments varies greatly, depending mainly on the exhaust temperature, noble metal and washcoat used in the oxidation catalyst. Based on their gaseous phase $H_2SO_4$ measurements in vehicle exhaust, Arnold et al. (2006) suggested that $\varepsilon$ can be enhanced to be as high as 90%. Similar conclusions have been made in other related studies (Maricq et al., 2002; Kittelson et al., 2006). Giechaskiel et al. (2007) have expressed $\varepsilon$ as function of exhaust temperature by compiling data from different studies. The relationship between $\varepsilon$ and the exhaust temperature used in this study has been adopted from Fig. 8 in Giechaskiel et al. (2007).

Although laboratory studies have indicated that the sulfuric acid is involved in the formation of observed nanoparticles under ultra-low sulfur conditions for vehicles equipped with advanced after-treatments such as CRDPFs, the theoretical assessment of this issue is yet to be performed. In order to understand whether BHN is the nucleation mechanism, we have carried out two case studies. The first one looks into the laboratory study by Vaaraslahti et al. (2005) which focused on the effect of lubricant oil on nanoparticle formation (FSC=1 ppm). In the second case study, on-road measurements by Kittelson et al. (2006), which studied the effect of diesel exhaust after-treatments on nanoparticle formation (FSC=15 ppm) have been simulated. Both studies were conducted with ultra-low sulfur fuels. Two-stage dilution system was used in Vaaraslahti et al. (2005), while the exhaust was diluted continuously in the work of Kittelson et al. (2006). The cut-off size of the particle size distribution in both measurements was ~3 nm. The key parameters of experimental setups such as exhaust temperature and dilution profile, ambient and dilution air temperature, sulfur content of fuel and lubricating oil were explicitly specified. The detailed experimental setups and key parameters can be found in (Vaaraslahti et al., 2005; Kittelson et al., 2006), and the corresponding parameters used to constrain the present model are given in Table 1.

Figure 1 shows the comparison of the simulated particle size distribution with the observed one from Vaaraslahti et al. (2005). $\varepsilon$ used in the simulations is assumed to be 100 % for exhaust temperature of 750 K. As seen from Fig. 1, the predicted parti-



cle size distribution is in good agreement with the measurement, especially in terms of mode peak concentration and mean size. Figure 2a shows the effect of the exhaust temperature on the particle ($Dp$>=3 nm) number concentration based on both model simulations and measurements. As seen from Fig. 2a, the predicted particle number concentration tracks the measured ones well over full range of the temperatures. It is important to note that the sulfur conversion efficiency at each exhaust temperature is a critically important parameter in the model simulation because it controls $H_2SO_4$ concentration in raw exhaust. In the view of the critical importance of the sulfur conversion efficiency, Fig. 2b compares the sulfur conversion efficiency used in the simulations at each exhaust temperature with those from Fig. 8 in Giechaskiel et al. (2007). As can be seen from Fig.2 b, the model-derived relationship of the sulfur conversion efficiencies as a function of the exhaust temperature is in good agreement with experimental data. This means that our model is capable of accurately predicting the temperature dependences of nucleation rates. This model may also be used to infer the temperature-dependent sulfur conversion efficiency of a particular CRDPF by fitting the predicted particle number concentrations to the measured ones.

The comparisons of the simulation results with measurements indicate that our model accurately predicts not only in the particle size distribution but also in the temperature dependence of nucleation rates. Moreover, the good agreement between the theory and experiments gives us a clear indication that BHN is responsible for the nanoparticle formation in the exhaust of vehicles with CRDPFs running on ultra-low sulfur fuel. These results are encouraging for the further applications of the developed model to the formation and evolution of nanoparticles in the vehicular exhaust diluting in the real atmosphere. Figure 3 shows the evolution of the particle size spectrum as a function of plume ages up to 75 s under (a) ultra-low sulfur conditions (effective sulfur content (ESC)=30 ppm with FSC=15 ppm and contribution from lube sulfur content (LSC)=15 ppm) and (b) high sulfur conditions (ESC=330 ppm with FSC=330 ppm) in a winter condition (T=278 K, RH=60%). LSC represents sulfur content from the lubricating oil and effective sulfur content is the sum of both FSC and LSC. It is important

to note that the sulfur from the lubricating oil has to be accounted for in the case when the ultra-low sulfur fuel is used. The LSC is assumed to be 3000 pm with lube oil leaking rate assumed to be 0.5% (Abdul-Khalek et al., 1998). The sulfur conversion efficiency is assumed to be 60% for Fig. 3a and 1.4% for Fig. 3b, respectively. Data shown in Fig. 3a were obtained assuming that CRDPFs efficiently removes all of organic compounds in exhaust. This is consistent with recent findings of Vaaraslahti et al. (2004) who have observed a reduction of 90% in total hydrocarbon concentration for a heavy duty diesel vehicle equipped with CRDPFs. The wind speed is assumed to be 2 m/s and the distance of vehicular plume away from centerline of highway is calculated based on the plume age. A distance of 12 m from centerline of the roadway is considered as a border of the roadside, assuming roadway to be totally 24 m in width.

As seen from Fig. 3a, no nucleation happens (dot-dashed curve in black) if vehicles are not equipped with CRDPFs and running with fuel with FSC=15 ppm; however, significant nucleation occurs when CRDPFs are functioning (solid curve in black). Mode I is composed exclusively of $H_2SO_4$-$H_2O$ particles formed via BHN nucleation. Mode III consists mainly of soot agglomerates and ambient particles. Our model shows that most of the nucleation happens within plume age of 0.1 s. The concentration of particles in Mode I decrease with time mainly due to the atmospheric dilution since then. In addition, a distinct nucleation mode is formed within less than 1 s. The similar time scale has also been observed by Rönkkö et al. (2006) which have shown that the aerosol nucleation mode has been formed within 0.45 s of plume age.

An apparent difference in the particle size distribution between (a) ultra-low sulfur and (b) high sulfur case is the existence of Mode II reported in many recent field measurements. An example of such on road measurements (from Kittelson et al., 2004) is given in Fig. 3b. This measurement has been chosen because FSC and ambient temperature assumed in our simulation are close to high FSC in Minnesota (∼300–400 ppm) and cold ambient temperature during the measurements (274 K to 286 K). Due to its large Kelvin Effect, only part of Mode I particles can be activated by semi- and low volatile organics and form the Mode II. It is clear from Fig. 3b that our model



is able to capture the main features of the observed on-road nucleation mode (Mode II). The mean size of Mode II is close to observed nucleation mode and predicted peak concentration is in a reasonable agreement with measured one.

Due to the absence of organics associated with the equipment of CRDPFs in the ultra-low sulfur case (Fig. 3a), the mean size of the nucleation mode (Mode I) is ∼3–4 nm that is much smaller than that shown in Fig. 3b (Model II). This finding is consistent with the measurements reported in Kittelson et al. (2006), which show that the mean sizes of the observed nucleation mode are ∼5 nm or smaller for most exhaust temperatures. Although the mean size of nucleation mode becomes smaller, the number concentration of nucleation mode (Mode I) under ultra-low sulfur conditions will be at least the same, if not higher, than that of (Mode I + Mode II) under high sulfur conditions due to the enhanced sulfur conversion efficiency and removal of soot agglomerates. This indicates that the effect of reduction in fuel sulfur content on minimizing the vehicular nanoparticle emission is offset by the employment of CRDPFs.

### 3.2 Effect of sulfate storage and release on nanoparticle formation

Besides oxidizing $SO_2$, the diesel oxidation catalyst and/or particulate filter can also adsorb sulfate. Sulfate can also deposit on tailpipe walls. Sulfate may be released due to the saturation of storage sites and/or passage of the high temperature exhaust due to the vehicle acceleration. The sulfate release leads to a considerable increase in the $H_2SO_4$ concentration in exhaust, which makes BHN under ultra-low sulfur conditions possible, even in the case when $\varepsilon$ is low (due to less catalyst oxidation efficiency associated with low exhaust temperature). In the present work, we investigate the extent to which such sulfate storage/release effects may influence the nanoparticle formation in ultra-low sulfur conditions. Assuming that the original $H_2SO_4$ concentration in exhaust to be $C_0$ and that resulting from the sulfur release effect to be $C_1$, the storage/release enhance factor (SREF) can be defined as $C_1/C_0$. Clearly, the bigger is the SREF, the higher is the $H_2SO_4$ concentration in raw exhaust.

It is difficult to predict the amount of sulfate deposited on exhaust after-treatments

or tailpipe, and no direct measurements on SREF are available at the present time. SREF depends on several factors, such as type and mass of washcoat, and exhaust temperature. Arnold et al. (2006) also attributed the occasionally measured high $\varepsilon$ to the release of sulfate from oxidation catalyst at high exhaust temperature. Since both the sulfur conversion process and the sulfate release effect may affect gaseous phase $H_2SO_4$ concentration, it is difficult to figure out whether it is enhanced oxidation or sulfate release that caused the observed high $\varepsilon$. However, we can get an upper limit of SREF which is calculated to be 10 based on Arnold et al.'s measurements by assuming that the sulfate release leads to the observed high $\varepsilon$,

Figure 4 shows the predicted nanoparticle emission indices as a function of SREF at 3 different $\varepsilon$s at two ambient temperatures (278 K and 298 K). The ESC is assumed to be 30 ppm. Two solid parallel lines from Zhang et al. (2005) represent lower and upper limits of the calculated nanoparticle emission index based on near road measurements (Zhu et al., 2002) in California. We consider any value above the lower line to be significant. In summertime, the sulfur release effect cannot produce the significant nanoparticles for the $\varepsilon$=2.5% case. However, this effect becomes important as $\varepsilon$ increases. SREF must have at least the value of 7 and 9 in order for BHN to produce significant amount of nanoparticles for cases of $\varepsilon$=5.0% and 3.5%, respectively. However, as ambient temperature decreases to 278 K, SREF needed to produce significant nanoparticles decreases by more than a factor of 2 for $\varepsilon$=3.5% and 5.0%. This suggests that the sulfur release effect on nanoparticle production become more significant in winter conditions.

### 3.3 Role of non-volatile cores in the formation of observed nanoparticles

A large number of systematic field measurements on the characterization of vehicle-emitted nanoparticles in California have been carried out in the past few years (Zhu et al., 2002, 2004, 2006; Kuhn et al., 2005a, b, c; Sardar et al., 2005; Westerdahl et al., 2005; Phuleria et al., 2007). While a lot of useful data on the particle size distribution, nanoparticle evolution process, and particle compositions have been reported,



little information on nanoparticle formation mechanism have been revealed. Although generally California fuel has FSC of ∼50 ppm, a key difference in nanoparticle formation between California case and ultra-low sulfur cases discussed earlier lies in the availability of CRDPFs. To our knowledge, no CRDPFs were employed during the time periods when those field campaigns were conducted. Low sulfur conversion efficiency is therefore expected for vehicles without CRDPFs. In order to address the questions-What could be the possible nanoparticle formation mechanism in California and could BHN be an essential nucleation source, we have applied the aerosol model to simulate nanoparticle formation under California conditions (i.e., low sulfur fuel and no CRDPFs) as to gain some insights into the nanoparticle formation mechanism. The presence of a mode of nanometer-sized non-volatile cores is considered. The existence of non-volatile cores has been long observed in a number of field and laboratory studies (Sakurai et al., 2003; Kittelson et al., 2006; Rönkkö et al., 2007). For example, Sakurai et al. (2003) pointed out that ∼12 and 30 nm particles did not completely evaporate even if they were heated up to ∼473 K and sizes of residual non-volatile cores were as small as ∼2–3 nm. The existence of non-volatile fractions of sampled nanoparticles have also been pointed out in their later field measurements (Kuhn et al., 2005; Biswas et al., 2007). In addition, Kittelson et al. (2006) observed a non-volatile mode with mean size of ∼10 nm at engine idle condition. More recently, Rönkkö et al. (2007) found that sampled nanoparticles consist of organic coated non-volatile cores which have been formed before the dilution process.

Figure 5a shows the evolution of nanoparticles as a function of the plume age with the assumed mode of non-volatile cores for vehicles running on low sulfur fuel (ESC=50 ppm with 35 ppm of FSC and 15 ppm of LSC). For the comparison purposes, a case without non-volatile cores is also shown (black-dashed line Fig. 5a). The non-volatile particles are assumed to be in the range of 1.8 nm-3 nm in diameter, which is consistent with recent measurements of Sakurai et al. (2003). The number concentration of non-volatile cores is assumed to be $3\times10^8$ cm$^{-3}$. It is important to note that the actual size range and concentrations of non-volatile core are expected to depend

strongly on soot concentration, engine operation conditions, and fuel and lube oil compositions (Rönkkö et al., 2007). No sulfur storage/release effect is considered in these simulations. For the assumed ESC and sulfur conversion efficiency, no nucleation mode particles were formed via BHN in the absence of non-volatile cores. This may indicate that BHN is not responsible for nanoparticle formation in California conditions. However, the presence of non-volatile cores leads to the formation of a clear nucleation mode with a mean size ~20 nm. The predicted particle size distribution is in reasonable agreement with observed on-road particle size distribution in Los Angeles by Westerhahl et al. (2005) at the ambient temperature of ~294 K. Our simulations show that most of the non-volatile cores are activated. We found that organic compounds, rather than $H_2SO_4$, are responsible for the activation of the non-volatile core mode. In the other words, $H_2SO_4$ concentration under low sulfur conditions (FSC=50 ppm) is not high enough to promote the growth of the non-volatile core mode to larger sizes that are ~20 nm. This finding is consistent with recent studies (Vaaraslahti et al., 2005; Rönkkö et al., 2007) which showed no clear effect of FSC on nucleation mode particles. This is different from cases of both high sulfur fuel and ultra-low sulfur fuel with CRDPFs. In those cases, nucleation mode is sensitive to FSC because of the high concentration of $H_2SO_4$ due to either the high fuel sulfur content or enhanced sulfur conversion efficiency or sulfur release effect.

Figure 5b shows the composition of particles of various sizes at 1 s of plume age. Similarly to the case of high sulfur content, organics contribute to the majority mass of the nucleation mode. The volume fraction of non-volatile cores is smaller than that of $H_2SO_4$ and accounts for less than 1% of total mass of nucleation mode particles. This is consistent with findings of Biswas et al. (2007) who showed that for 20 nm particles, non-volatile cores account for less than 3% of particle mass. Although the contribution of non-volatile cores to the nanoparticle mass is negligible, they are a source of the observed nucleation modes. It is important to note that the entire nucleation mode will still disappear (i.e., become undetectable) when these particles are passed through a thermal denuder due to the small mass fraction of solid component. In the other words,



a complete disappearance of entire observed nucleation mode may not necessarily be an indicator of absence of nanometer-sized non-volatile cores.

## 4 Summary and Discussion

A comprehensive modeling study of possible causes of nanoparticle formation under ultra-low sulfur conditions has been carried out using a size- and composition-resolved aerosol microphysics model with updated binary homogeneous nucleation (BHN) scheme. A good agreement of the predicted particle size distribution and temperature dependences of nucleation rates with experiments leads us to conclude that BHN is the nucleation mechanism of nanopaticle formation for vehicles equipped with CRDPFs and running on ultra-low sulfur fuel. We have shown that such vehicles emit at least the same, if not higher, number concentrations of nanoparticles than those without CRDPFs and running on high sulfur fuel. We also found that the sulfate storage/release effect can lead to a significant nanoparticle production under favorable conditions. This effect becomes more significant as the ambient temperature decreases. These findings lead us to conclude that although CRDPFs are effective in reducing the mass of vehicular emissions, they offset the positive effects of the reduced fuel sulfur contents on the nanoparticle formation and significantly enhance the number concentrations of nanoparticles in vehicular emissions. Moreover, higher nanoparticle number concentrations are expected when the enhanced sulfur conversion and sulfur release effect takes place simultaneously.

A complete physical picture of the nanoparticle formation and evolution on and near roadway has been also presented. Our simulations showed that most of nucleation events happen within 0.1 s of plume age and that a clear nucleation mode is developed within 1 s of plume age. Coagulation and dilution with or without organic condensation can change the particle size distribution at latter stages. We found that the mean size of nucleation mode becomes smaller because the total organic carbon concentration in raw exhaust can be significantly removed by CRDPFs. Smaller in size but of high num-

ber concentration, the nucleation mode has the lifetime of ∼300 s due to scavenging by ambient aerosol. The ambient existing particle number concentration of $10^4(cm^{-3})$ and coagulation kernel of $\sim 3\times10^{-7}(cm^3/s)$ of nanoparticles (∼2–3 nm) with larger soot or ambient particles (∼100 nm) due to Brownian motion at room temperature were used in the calculations. The present results lead us to conclude that the vehicle-emitted nanoparticles will affect not only residents living near the roadways but also those who live several hundreds meters away. The strength of the effect also depends on wind speed and atmospheric dilution.

In addition, we have shown that instead of BHN, the non-volatile cores are the source of observed nucleation mode in California, where low sulfur fuel is used and vehicles are not equipped with CRDPFs. We found that organics, rather than $H_2SO_4$, contribute to the growth of non-volatile particles that may explain the observed on-road nucleation mode. Non-volatile cores that are as small as ∼2–3 nm in diameter are able to grow to sizes larger than 10 nm by taking up the low and semi-volatile organics. No valuable information on the formation mechanism of these non-volatile cores is available at the present time. Recent studies suggest that non-volatile cores may be formed due to nucleation of metal oxides or heavy hydrocarbons inside the engine cylinder (Vaaraslahti et al., 2004; Kittelson et al., 2006). Their formation also depends on the engine load and availability of CRDPFs because non-volatile cores were often observed at low engine loads for vehicles without CRDPFs. Kittelson et al. (2006) suggest that low soot surface areas resulting from low engine loads may promote the metal oxide nucleation inside cylinder. Further research is needed to investigate the formation of the nanometer-sized non-volatile cores.

*Acknowledgements.* This work was supported by the National Science Foundation under grant ATM 0618124 and the New York State Energy Resource and Development Agency.



## References

Arnold, F., Pirjola, L., Aufmhoff, H., Schuck, T., Lahde, T., and Hameri, K.: First gaseous sulfuric acid measurements in automobile exhaust: Implications for volatile nanoparticle formation, Atmos. Environ., 40, 7097–7105, 2006.

Biswas, S., Ntziachristos, L., Moore, K. F., and Sioutas, C.: Particle volatility in the vicinity of a freeway with heavy-duty diesel traffic, Atmos. Environ., 41, 3479–3493, 2007.

Carbajal-Arroyo, L., Barraza-Villarreal, A., Durand-Pardo, R., Moreno-Macias, H., Espinoza-Lain, R., Chiarella-Ortigosa, P., and Romieu, I.: Impact of traffic flow on the asthma prevalence among school children in Lima, Peru, J. Asthma, 44, 197–202, 2007.

Kittelson, D. B., Kadue, P. A., Scherrer, H. C., and Loverien, R. E.: Characterization of diesel particle in the atmosphere, CRC, AP-2 Project Group, 1988.

Du, H. and Yu, F.: Role of the binary $H_2SO_4$-$H_2O$ homogeneous nucleation in the formation of volatile nanoparticles in the vehicular exhaust, Atmos. Environ., 40, 7579–7588, 2006.

Gauderman, W. J., Vora, H., McConnell, R., Berhane, K., Gilliland, F., Thomas, D., Lurmann, F., Avol, E., Kunzli, N., Jerrett, M., and Peters, J.: Effect of exposure to traffic on lung development from 10 to 18 years of age: a cohort study, Lancet, 369, 571–577, 2007.

Giechaskiel, B., Ntziachristos, L., Samaras, Z., Casati, R., Scheer, V., and Vogt, R.: Effect of speed and speed-transition on the formation of nucleation mode particles from a light duty diesel vehicle, SAE J-Automot. Eng., 01, 1110, 307–319, 2007.

Hanson, D. R. and Lovejoy, E. R.: Measurement of the thermodynamics of the hydrated dimer and trimer of sulfuric acid, J. Phys. Chem. A, 110, 9525–9528, 2006.

I. S. Abdul-Khalek, D. B. Kittelson, B. R. Graskow, Q. Wei, and Brear, F.:
Diesel exhaust particle size: Measurement issues and trends, SAE J-Automot. Eng., 980525, 81–93, 1998.

Seinfeld, J. H. and Pandis, S. N.: Atmospheric Chemistry and Physics: From Air Pollution to Climate Change, New York, NY, Wiley, 1998.

Jacobson, M. Z., Kittelson, D. B., and Watts, W. F.: Enhanced coagulation due to evaporation and its effect on nanoparticle evolution, Environ. Sci. Technol., 39, 9486–9492, 2005.

Kittelson, D. B., Watts, W. F. and Johnson, J. P.: Nanoparticle emissions on Minnesota highways, Atmos. Environ., 38, 9-19, 2004.

Kittelson, D. B., Watts, W. F. and Johnson, J. P.: On-road and laboratory evaluation of combustion aerosols–Part1: Summary of diesel engine results, J. Aerosol Sci., 37, 913-930,

2006.
Kittelson, D. B., Watts, W. F., Johnson, J. P., Rowntree, C., Payne, M., Goodier, S., Warrens, C., Preston, H., Zink, U., Ortiz, M., Goersmann, C., Twigg, M. V., Walker, A. P., and Caldow, R.: On-road evaluation of two Diesel exhaust aftertreatment devices, J. Aerosol Sci., 37, 1140–1151, 2006.
Kuhn, T., Biswas, S., Fine, P. M., Geller, M., and Sioutas, C.: Physical and chemical characteristics and volatility of PM in the proximity of a light-duty vehicle freeway, Aerosol Sci. Tech., 39, 347–357, 2005a.
Kuhn, T., Biswas, S., and Sioutas, C.: Diurnal and seasonal characteristics of particle volatility and chemical composition in the vicinity of a light-duty vehicle freeway, Atmos. Environ., 39, 7154–7166, 2005b.
Kuhn, T., Krudysz, M., Zhu, Y., Fine, P. M., Hinds, W. C., Froines, J., and Sioutas, C.: Volatility of indoor and outdoor ultrafine particulate matter near a freeway, J. Aerosol Sci., 36, 291–302, 2005c.
Makar, P. A.: The estimation of organic gas vapour pressure, Atmos. Environ., 35, 961–974, 2001.
Maricq, M. M., Chase, R. E., Xu, N., and Laing, P. M.: The Effects of the Catalytic Converter and Fuel Sulfur Level on Motor Vehicle Particulate Matter Emissions: Light Duty Diesel Vehicles, Environ. Sci. Technol., 36, 283–289, 2002.
Meng, Y. Y., Wilhelm, M., Rull, R. P., English, P. and Ritz, B.: Traffic and outdoor air pollution levels near residences and poorly controlled asthma in adults, Ann. Allerg. Asthma Im., 98, 455-463, 2007.
Phuleria, H. C., Sheesley, R. J., Schauer, J. J., Fine, P. M., and Sioutas, C.: Roadside measurements of size-segregated particulate organic compounds near gasoline and diesel-dominated freeways in Los Angeles, CA, Atmos. Environ., 41, 4653–4671, 2007.
Rönkkö, T., Virtanen, A., Kannosto, J., Keskinen, J., Lappi, M., and Pirjola, L.: Nucleation mode particles with a nonvolatile core in the exhaust of a heavy duty diesel vehicle, Environ. Sci. Technol., 41, 6384–6389, 2007.
Rundell, K. W., Hoffman, J. R., Caviston, R., Bulbulian, R., and Hollenbach, A. M.: Inhalation of ultrafine and fine particulate matter disrupts systemic vascular function, Inhal. Toxicol., 19, 133–140, 2007.
Sakurai, H., Tobias, H. J., Park, K., Zarling, D., Docherty, K. S., Kittelson, D. B., McMurry, P. H., and Ziemann, P. J.: On-line measurements of diesel nanoparticle composition and volatility,



Atmos. Environ., 37, 1199–1210, 2003.
Sardar, S. B., Fine, P. M., Mayo, P. R. and Sioutas, C.: Size-fractionated measurements of ambient ultrafine particle chemical composition in Los Angeles using the NanoMOUDI, Environ. Sci. Technol., 39, 932–944, 2005.
Shi, J. P., Harrison, R. M., Evans, D. E., Alam, A., Barnes, C., and Carter, G.: A Method for measuring particle number emissions from vehicles driving on the road, Environ. Technol., 23, 1–14, 2002.
Vaaraslahti, K., Keskinen, J., Giechaskiel, B., Solla, A., Murtonen, T., and Vesala, H.: Effect of lubricant on the formation of heavy-duty diesel exhaust nanoparticles, Environ. Sci. Technol., 39, 8497–8504, 2005.
Vaaraslahti, K., Virtanen, A., Ristimaki, J., and Keskinen, J.: Nucleation mode formation in heavy-duty diesel exhaust with and without a particulate filter, Environ. Sci. Technol., 38, 4884–4890, 2004.
Westerdahl, D., Fruin, S., Sax, T., Fine, P. M., and Sioutas, C.: Mobile platform measurements of ultrafine particles and associated pollutant concentrations on freeways and residential streets in Los Angeles, Atmos. Environ., 39, 3597–3610, 2005.
Wold, L. E., Simkhovich, B. Z., Kleinman, M. T., Nordlie, M. A., Dow, J. S., Sioutas, C., and Kloner, R. A.: In vivo and in vitro models to test the hypothesis of particle-induced effects on cardiac function and arrhythmias, Cardiovasc. Toxicol., 6, 69–78, 2006.
Yu, F.:From molecular clusters to nanoparticles: Second-generation ion-mediated nucleation model, Atmos. Chem. Phys.,6, 5193-5211, 2006.
Yu, F.:Improved quasi-unary nucleation model for binary $H_2SO_4$-$H_2O$ homogeneous nucleation, J. Chem. Phys., 127, 054301, 2007.
Zhang, K. M., Wexler, A. S., Zhu, Y. F., Hinds, W. C., and Sioutas, C.: Evolution of particle number distribution near roadways. Part II: The 'Road-to-Ambient' process, Atmos. Environ., 38, 6655–6665, 2004.
Zhu, Y., Hinds, W. C., Kim, S., Shen, S., and Sioutas, C.: Study of ultrafine particles near a major highway with heavy-duty diesel traffic, Atmos. Environ., 36, 4323–4335, 2002.
Zhu, Y., Hinds, W. C., Shen, S., and Sioutas, C.: Seasonal trends of concentration and size distribution of ultrafine particles near major highways in Los Angeles, Aerosol Sci. Tech., 38, 5–13, 2004.

Zhu, Y., Kuhn, T., Mayo, P., and Hinds, W. C.: Comparison of daytime and nighttime concentration profiles and size distributions of ultrafine particles near a major highway, Environ. Sci. Technol., 40, 2531–2536, 2006.



**Table 1.** Parameters used for comparisons of model simulation with laboratory studies (Vaaraslahti et al., 2005; Kittelson et al., 2006)

| | Kittelson et al. (2006) | Vaaraslahti et al. (2005) |
|---|---|---|
| fuel sulfur content (ppm) | 15 | 1 |
| lubricant sulfur content (ppm) | 1300 | 5100 |
| lube oil consumption rate (%) | 0.5 | 0.5 |
| exhaust temperature (K) | 603.15–643.15 | 750.15 |
| dilution air temperature (K) | 295.15 | 303.15 |
| Dilution ratio | 400–600 | Primary 12, secondary 8 |
| residence time (s) | 1 s in air, 2 s in sampling line | 3 s in ageing chamber |

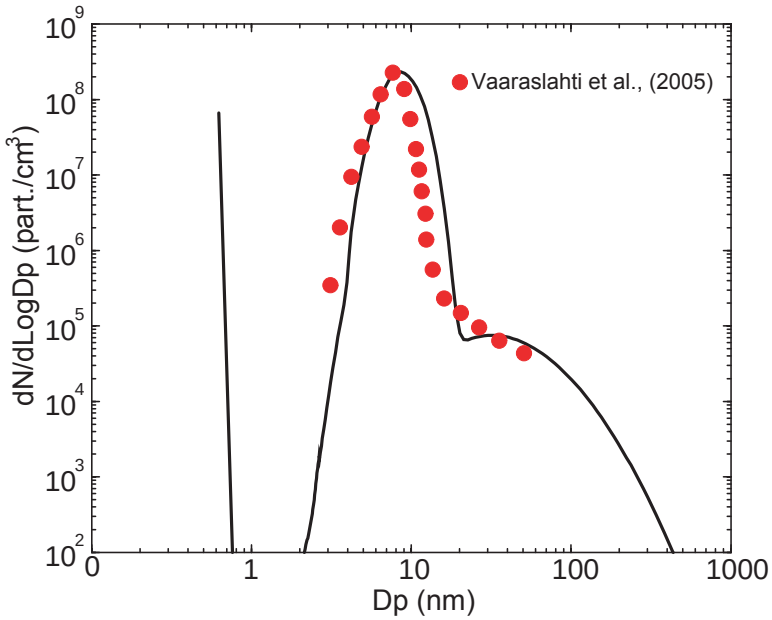


**Fig. 1.** Comparison between the predicted particle size distribution and measured one from Vaaraslahti et al. (2005). The sulfur to sulfuric acid conversion efficiency $\varepsilon$ used in the simulation is assumed to be 100% for exhaust temperature of 750 K.



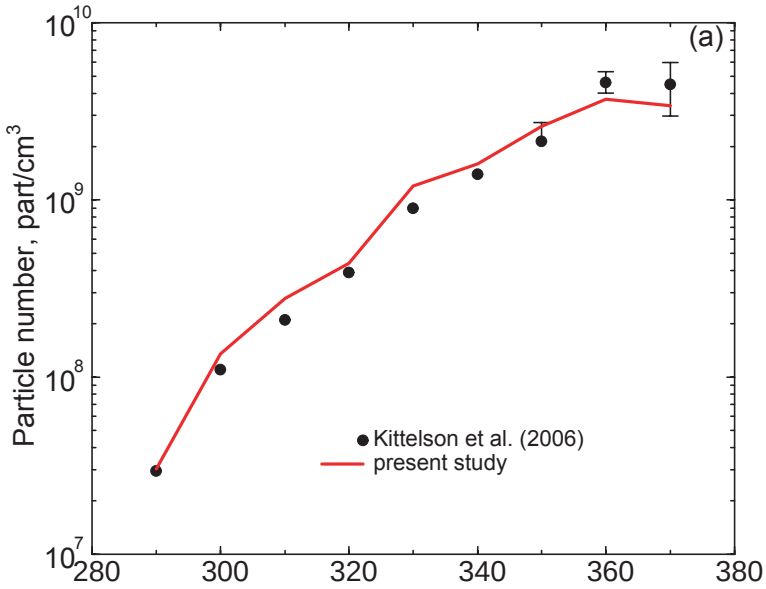


**Fig. 2a.** The effect of exhaust temperatures on **(a)** dilution corrected number concentrations of nanoparticles ($Dp$>3 nm) formed in the vehicle equipped with modern diesel particle filters, and **(b)** sulfur to sulfuric acid conversion efficiency assumed in our simulation and from other studies. The experimental data (black dots) in Fig. 2a are from (Kittelson et al., 2006). The sulfur conversion efficiencies are adjusted in the model so that the predicted nanoparticle concentrations are close to the measured ones for different exhaust temperatures. The sulfur conversion efficiencies inferred in this way along with numbers reported in other studies are plotted in Fig. 2b as function of exhaust temperature.

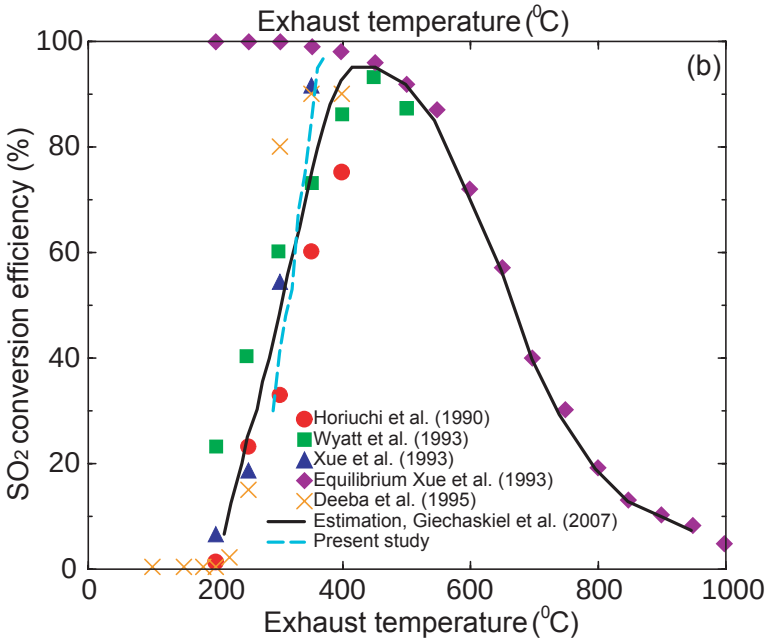


**Fig. 2b.** Continued.



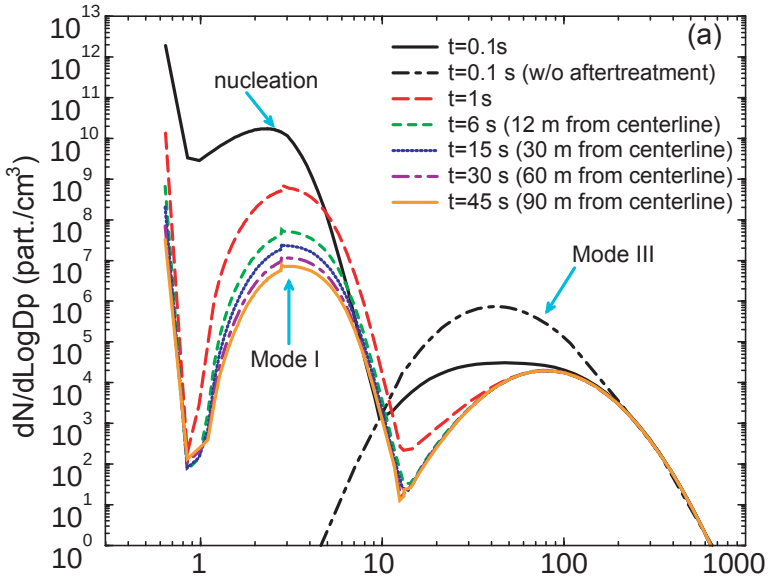


**Fig. 3a.** Nanoparticle formation and evolution as a function of plume ages up to 75 s under **(a)** ultra-low sulfur conditions (effective sulfur content ESC=30 ppm) and **(b)** high sulfur conditions (ESC=330 ppm) in a winter condition (T=278 K, RH=60%). The sulfur conversion efficiency is assumed to be 60% for Fig. 3a and 1.4% for Fig. 3b, respectively. Particle number concentration is not corrected for dilution.

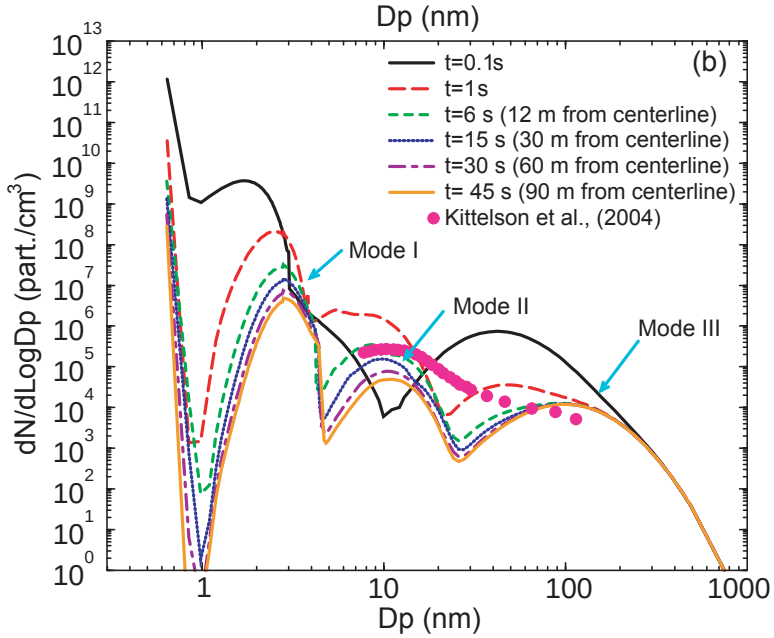


**Fig. 3b.** Continued.



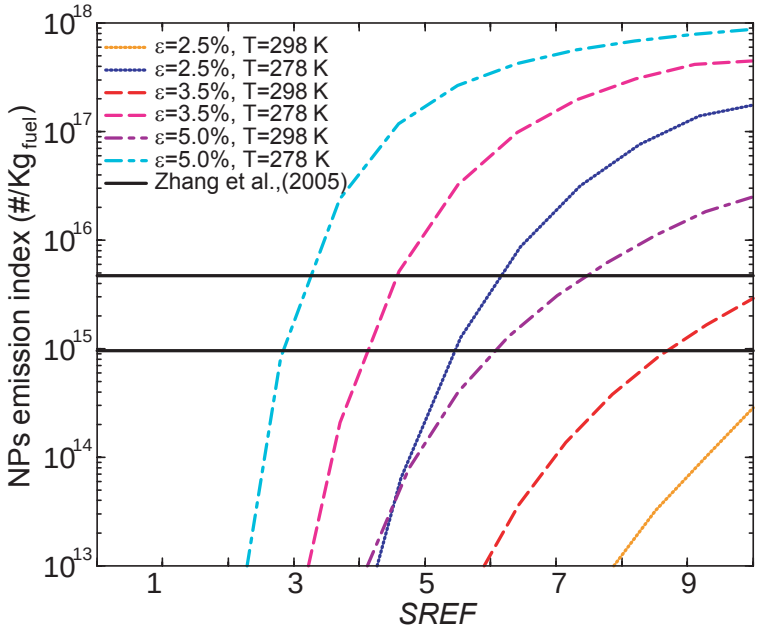


**Fig. 4.** Dependence of dilution corrected nanoparticle emission indices on SREF at 3 different $\varepsilon$s (2.5%, 3.5%, and 5.0%) at ambient RH=50% in winter ($T$=278 K) and summer ($T$=298 K) conditions. The ESC is assumed to be 30 ppm.

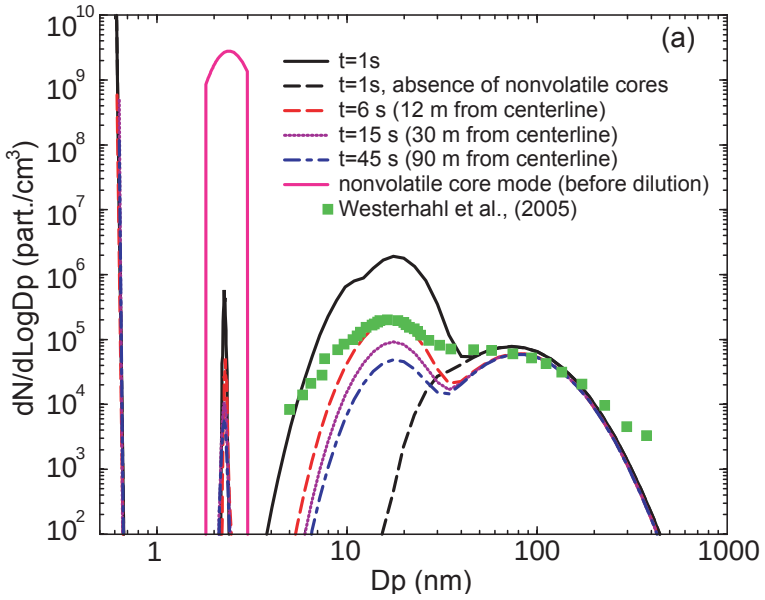


**Fig. 5a.** **(a)** Evolution of nanoparticle size distributions at four selected plume ages with the presence of non-volatile cores, and **(b)** volume size distributions for different components at plume age of 1 s. The ambient T and RH are 295 K and 60%, respectively. ESC=50 ppm and $\varepsilon$=2.5%. The particle number and volume size distribution is not corrected for dilution.



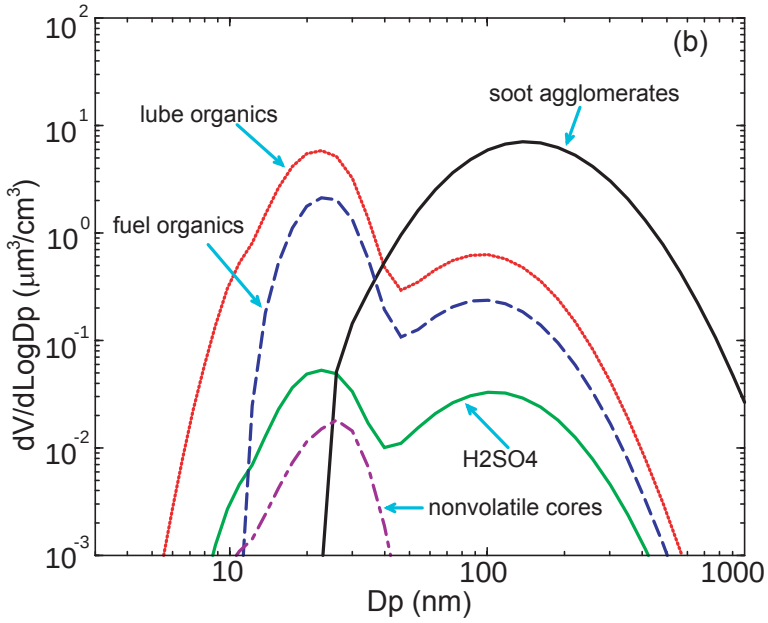


**Fig. 5b.** Continued.